Received: 26 September 2020 | Revised: 1 March 2021 | Accepted: 24 March 2021

DOI: 10.1002/jor.25050

RESEARCH ARTICLE

Journal of Orthopaedic Research®

Painful temporomandibular joint overloading induces structural remodeling in the pericellular matrix of that joint's chondrocytes

Melissa Franklin[1] | Megan M. Sperry[2] | Evan Phillips[3] | Eric J. Granquist[4] | Michele Marcolongo[3] | Beth A. Winkelstein[2]

[1]School of Biomedical Engineering, Science, and Health Systems, Drexel University, Philadelphia, Pennsylvania, USA

[2]Department of Bioengineering, University of Pennsylvania, Philadelphia, Pennsylvania, USA

[3]Department of Materials Science and Engineering, Drexel University, Philadelphia, Pennsylvania, USA

[4]Oral and Maxillofacial Surgery, University of Pennsylvania, Philadelphia, Pennsylvania, USA

Correspondence
Megan M. Sperry, Wyss Institute at Harvard University, 3 Blackfan Cir, Boston, MA 02115, USA.
Email: megan.sperry@wyss.harvard.edu

Funding information
Catherine D. Sharpe Foundation; Oral and Maxillofacial Surgery Foundation; National Science Foundation, Grant/Award Number: #1826202; National Institute of Arthritis and Musculoskeletal and Skin Diseases, Grant/Award Number: T32-AR007132; Oral and Maxillofacial Surgery Schoenleber Research Fund

Abstract

Mechanical stress to the temporomandibular joint (TMJ) is an important factor in cartilage degeneration, with both clinical and preclinical studies suggesting that repeated TMJ overloading could contribute to pain, inflammation, and/or structural damage in the joint. However, the relationship between pain severity and early signs of cartilage matrix microstructural dysregulation is not understood, limiting the advancement of diagnoses and treatments for temporomandibular joint-osteoarthritis (TMJ-OA). Changes in the pericellular matrix (PCM) surrounding chondrocytes may be early indicators of OA. A rat model of TMJ pain induced by repeated jaw loading (1 h/day for 7 days) was used to compare the extent of PCM modulation for different loading magnitudes with distinct pain profiles (3.5N—persistent pain, 2N—resolving pain, or unloaded controls—no pain) and macrostructural changes previously indicated by Mankin scoring. Expression of PCM structural molecules, collagen VI and aggrecan NITEGE neo-epitope, were evaluated at Day 15 by immunohistochemistry within TMJ fibrocartilage and compared between pain conditions. Pericellular collagen VI levels increased at Day 15 in both the 2N ($p = 0.003$) and 3.5N ($p = 0.042$) conditions compared to unloaded controls. PCM width expanded to a similar extent for both loading conditions at Day 15 (2N, $p < 0.001$; 3.5N, $p = 0.002$). Neo-epitope expression increased in the 3.5N group over levels in the 2N group ($p = 0.041$), indicating pericellular changes that were not identified in the same groups by Mankin scoring of the pericellular region. Although remodeling occurs in both pain conditions, the presence of pericellular catabolic neo-epitopes may be involved in the macrostructural changes and behavioral sensitivity observed in persistent TMJ pain.

KEYWORDS
collagen, joint overloading, osteoarthritis, pericellular matrix, temporomandibular joint

1 | INTRODUCTION

Temporomandibular joint disorders (TMDs) are the second-most common source of orofacial pain.[1] A substantial subset of patients with TMD develop osteoarthritis (OA), which is characterized by intra-articular inflammation and cartilage degeneration.[2] Macroscopic changes observed with temporomandibular joint-OA (TMJ-OA) include changes in joint shape and size, decreased condylar cartilage volume, and thickened articular disc and surrounding fossa.[3,4] There is a known association between osteoarthritic-related symptomatic pain and tissue degeneration.[2,5–8] However, differential diagnoses and treatments for patients experiencing latent pain and those who develop chronic, active orofacial pain remain a clinical challenge. Accordingly, studying the relationship between pain and changes in tissue structure that are characteristic of TMJ-OA is needed.

OA pathology involves alteration in the catabolic, inflammatory, and structural molecular components of the condylar cartilage tissue, which consists of chondrocytes.[2,5,9,10] The pericellular matrix (PCM) surrounds chondrocytes within the temporomandibular condyle and plays an important role in mechanotransduction, cytoprotection, and biochemical signaling.[10–13] The PCM consists of densely packed collagens and proteoglycans, including collagen VI and aggrecan, each with critical roles in maintaining the PCM's structural integrity. Collagen VI serves as a mechanical tether and protective layer surrounding chondrocytes,[14,15] whereas aggrecan is primarily responsible for regulating hydration, swelling, and supporting compression[16–19] (Figure 1B). Recently, PCM microstructural changes have been suggested to compromise chondrocyte mechanical properties[20] and serve as early indicators for OA progression.[21]

The structural and morphological changes associated with osteoarthritic cartilage are often assessed by the well-established Mankin grading system.[22] That technique evaluates the overall health of the cartilage tissue using grading of the intensity of histologically stained cartilage, including categorizing the label intensity of the PCM.[23,24] Although accepted as a reliable tool to study TMJ-OA,[22–24] there are constraints with Mankin scoring not being able to provide a detailed view of histological outcomes, especially within localized regions like the dynamic PCM.[21,25] In experimental models of OA that target specific markers within the PCM, there is evidence that collagen VI levels increase and become more distributed throughout the tissue matrix.[26,27] It is also well accepted

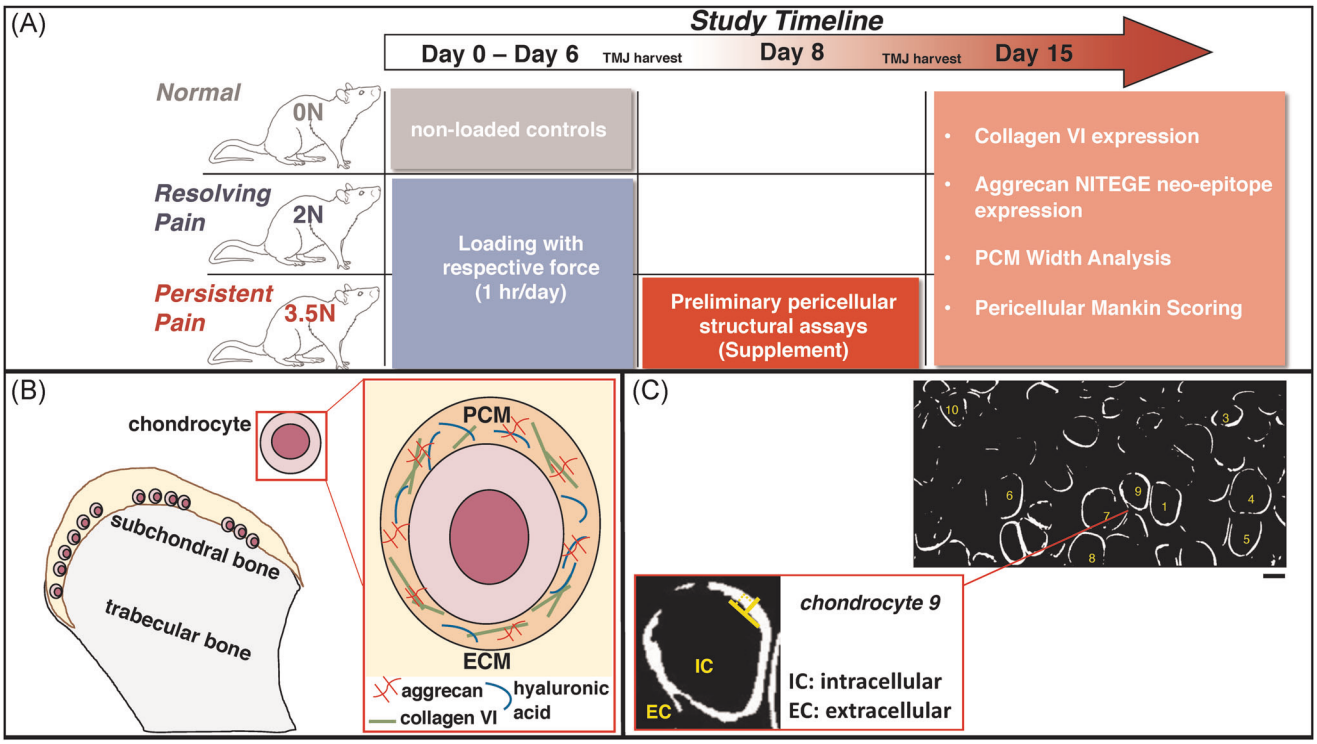

FIGURE 1 Summarized Methods Panel. (A) Overview of the study timeline: the repeated loading period occurred from Day 0 to Day 6 to induce tunable pain; an early pericellular structural assessment was performed on harvested TMJs within the 3.5N-loaded group at Day 8; and all experimental groups' pericellular structural assays were completed at Day 15. (B) Illustration of the PCM within TMJ cartilage. Our study focuses on the evaluation of collagen VI fibrillar protein and fragments of bottlebrush-shaped aggrecan proteoglycan attachments following painful loading. (C) An example image of hypertrophic chondrocytes and measurement technique for pericellular width quantification via collagen VI marker guidance. (*top*) TMJ sections labeled for collagen VI were converted to bifiltered images through MATLAB. Ten randomly selected chondrocytes from each image (two images per animal) were measured. The location of measurement along the PCM (in white) was also randomly selected. Scale bar = 10 μm. (*bottom*) Expanded view of a single chondrocyte displaying inner and outer boundaries and perpendicular direction (⊥) of manual width measurement completed via ImageJ. PCM, pericellular matrix; TMJ, temporomandibular joint [Color figure can be viewed at wileyonlinelibrary.com]

that aggrecan depletion is characteristic of osteoarthritic development in other joint models.[16–18,28–31] Together, organizational changes in collagen VI and aggrecan biomarkers destabilize the PCM and contribute to the onset of OA and mediate disease severity.[28,32,33] Further, while the Mankin score remains popular for its adaptability to several animal species and human cartilage models,[22] the scoring system's accuracy has not been compared to the use of pericellular marker labeling to detect early TMJ-OA progression.

This study sought to evaluate the extent of pericellular structural modulation in the TMJ using a tunable rat model of TMJ pain that is induced by repeated loading of the jaw (Figure 1A), and that has been well-characterized for its painful behavioral outcomes, as well as inflammatory and catabolic cascades representative of TMJ-OA pathomechanisms.[2,25,35,36] Previous work with this model graded orofacial expression through the Rat Grimace Scale (RGS) to score affective TMJ pain and mechanical reflex responses, defining a threshold for evoked peripheral sensitivity.[34] Briefly, a 2N load of repeated mouth-opening induces resolving pain, whereas a greater 3.5N of force induces persistent pain behaviors[2,34,35] (Figure 1A). Further, TMJs from both loading paradigms were previously characterized by the Mankin scoring system, and only the 3.5N-loaded persistent pain condition was found to exhibit significant tissue structural changes at Day 15.[34] In the present study, changes in the pericellular collagen VI protein and aggrecan NITEGE neo-epitope were evaluated at Day 15 for both the resolving and persistent pain conditions.

Our central hypothesis is that collagen VI and aggrecan neo-epitope expression and distribution will increase in painful, overloaded TMJs compared to unloaded controls, with the greatest extent of pericellular remodeling occurring in TMJs that develop persistent sensitivity. Collagen VI is expected to increase since chondrocytes upregulate protein synthesis to preserve PCM tethering and protect against further degradation. Furthermore, we expect increased aggrecan fragmentation (i.e., expression of neo-epitope) in the TMJ cartilage since it is an initial indication of degradation and subsequent proteoglycan loss characteristic of OA. Characterizing PCM molecule expression and distribution will help identify whether there is degradation and provide detailed insight into the tissue structural outcomes of TMJ-OA. In addition, this investigation begins to define a relationship between a painful mechanical overloading paradigm and pericellular changes characteristic of TMJ-OA onset and progression.

2 | METHODS

2.1 | Mechanical loading of rat TMJ

All studies used adult, weight-matched (277.50 ± 4.24 g) and age-matched (70–80 days following receipt) female Holtzman rats (Envigo). Rats were housed in groups of 2–3 in standard polycarbonate caging (AnCare), with 0.25-inch corncob bedding (Bed-o'Cobs; The Andersons Lab Bedding Products) and ad libitum access to food (LabDiet 5001; LabDiet) and water (acidified to pH = 3). Rats were housed in an Association for Assessment and Accreditation of Laboratory Animal Care accredited vivarium under a 12:12 h light:-dark cycle in a temperature-controlled environment in accordance with recommendations set forth in The Guide for Care and Use of Laboratory Animals (8th edition).[36] All animal procedures were approved by the IACUC at the University of Pennsylvania (IACUC #803831) and adhered to research and ethical guidelines of the International Association for Study of Pain.[37] Rats were exposed in separate, randomized groups to daily repeated mechanical loading of the jaw under isoflurane anesthesia at 2N (induces resolving orofacial sensitivity) and 3.5N (induces persistent orofacial sensitivity) for 1 h each day for 7 days[2,34,35] (Figure 1A). All mechanically loaded TMJs were compared to control TMJs from rats that did not receive loading (normal). For all tissue harvests, rats were deeply anesthetized with pentobarbital (65 mg/kg) and perfused with phosphate buffer saline (PBS).

2.2 | TMJ behavioral sensitivity assessment

Mechanical reflex testing in the temporomandibular joint region was used to determine the extent of temporomandibular pain for each loading magnitude. Joint sensitivity reflex tests were performed at baseline (before loading), every other day during (Days 1, 3, 5), and after the loading period (Days 7, 9, 11, 13, and 14) for rats exposed to 2 or 3.5N loading. Sensitivity measurements were acquired in the morning before that day's loading. The threshold for eliciting a head withdrawal was measured using von Frey filaments of increasing strengths from 0.6 to 60 g to stimulate the TMJ region (Stoelting).[38] This assessment for pain sensitivity was performed on the subset of rats used for Day 15 pericellular structural assays in this study ($n = 7$/group). A separate analysis compared the 3.5N-loaded animals in Day 8 and Day 15 tissue groups ($n = 5$/group). Head withdrawal thresholds were averaged across each group, log-transformed to normalize distribution, then compared used a repeated-measures analysis of variance with a post hoc Sidak's multiple comparisons test ($\alpha = 0.05$).[2,34,35]

2.3 | TMJ tissue preparation

To assess collagen VI expression, rats from the no loading, 2N, and 3.5N groups ($n = 5$/group) were fixed by 4% paraformaldehyde, and TMJs were harvested en bloc at Day 15. All fixed TMJs were stored in 30% sucrose in PBS and later decalcified with 0.25 M EDTA for 3 weeks at 4°C. A separate set of fixed TMJs ($n = 5$ rats) were also harvested at Day 8 from the 3.5N loading condition. To assess aggrecan NITEGE neo-epitope expression, TMJs were harvested unfixed freshly from the no loading, 2N, and 3.5N groups at Day 15 ($n = 4$ rats/group), immediately placed in 10% protease inhibitor cocktail in PBS to avoid protein degradation and stored at −20°C. Table 1 summarizes the experimental groups and assessments completed in this study.

TABLE 1 Summary of pericellular structural assays and examined conditions

Assessment	Day 8	Day 15
Collagen VI (n = 5/group)	3.5N (Figure S3)	2N, 3.5N
Aggrecan neo-epitope (n = 4/group)	---	2N, 3.5N
Pericellular width analysis (n = 5/group)	---	2N, 3.5N
Pericellular Mankin scoring (n = 4/group)	3.5N (Figure S4)	2N, 3.5N

2.4 | Immunohistochemistry and immunofluorescence labeling

Fixed TMJs were embedded in Tissue–Tek OCT compound (Sakura Finetek) and sagittally sectioned. Fixed TMJ sections used for immunohistochemistry (IHC) were sectioned at 18 μm, and thaw-mounted onto slides. IHC was performed via incubating sections with primary antibody against collagen VI (1:1250; Fitzgerald) or aggrecan NITEGE neo-epitope (1:1000; Thermo Fisher Scientific) overnight at 4°C. After washing, sections were incubated with biotinylated horse anti-rabbit secondary (1:1,000; Vector Laboratories) for 2 h, developed using 3,3′-diaminobenzidine (DAB), and cover-slipped. For collagen VI expression assessment, two histological sections of each DAB-IHC TMJ sample were imaged at ×40 using the EVOS FL Auto Imaging System (Thermo Fisher Scientific). Fresh TMJs used for immunofluorescence evaluation were similarly embedded, then sectioned at 5 μm with direct adherence to Kawamoto's sectioning tape. Sections were incubated for 30 min at room temperature using the same primary antibodies with higher concentrations (1:50 and 1:25 for collagen VI and NITEGE neo-epitope, respectively). The secondary label was then applied to sections for 30 min using goat anti-rabbit AlexaFlour 488. For aggrecan neo-epitope expression assessment, two histological sections of each IF-IHC labeled TMJ were imaged using confocal microscopy (Leica® TCS SP8 Multiphoton Confocal; ×63 magnification; 15% laser intensity, 850 V gain).

2.5 | Quantification of pericellular marker expression

Collagen VI expression was quantified using DAB-IHC images. Images were cropped to an approximated depth within the fibrocartilage tissue (150–200 μm)[28] and at standardized image dimensions (1000 × 500 pixels) to include the deep-hypertrophic zone. This zone was selected for analysis because it is proteoglycan-rich, and since resistance to compression is largely dictated by proteoglycan-collagen networks, this region is suggested to show a stronger response to applied loads[39] and cause the earliest mechanical matrix imbalances associated with TMJ-OA compared to the superficial, fibrous layers.[40–42] A custom MATLAB script measured collagen VI expressions as a percentage of surface area.[43] Following percent positive pixels analysis of collagen VI expression for each experimental group and unloaded controls, an additional average PCM width analysis was performed manually to quantify the extent of pericellular expansion following loading conditions using ImageJ with collagen VI as guidance marker (Figure 1C). Width measurements were derived from the MATLAB-processed, bi-filtered images and were taken at a perpendicular angle from the inner-most boundary (interfacing intracellular space) to the outer-most boundary (interfacing the extracellular space) of a chondrocyte's PCM ring. Each TMJ sample had two images that underwent PCM width analysis, where the pericellular width was averaged from 10 randomized chondrocytes per image.

Aggrecan NITEGE neo-epitope expression was quantified from IF-IHC images cropped to the deep-hypertrophic zone at standardized dimensions (900 × 350 pixels), and the labeled area was measured using the same MATLAB code to calculate the percentage of surface area. Separate one-way analysis of variances (ANOVAs) and post hoc Tukey tests ($\alpha = 0.05$) were performed to determine significance for each expression characterization and for PCM width analysis.

2.6 | Pericellular Mankin scoring from Safranin-O/Fast Green histological images

Global cartilage structure was evaluated using previously published methods.[34] Briefly, TMJs were stained by Safranin-O/Fast Green, imaged by widefield microscopy, and evaluated for the extent of cartilage degradation by two blinded observers using the modified Mankin scale.[23,24] The global Mankin scoring evaluated four subcategories including pericellular and background Safranin-O/Fast Green labeling, chondrocyte arrangement, and structural condition of the cartilage, ranging from a combined score of 0 representing normal cartilage to a maximum of 10 for severely degenerated cartilage totaled from subscores from the subcategories.[23,24,34] This investigation focused on the pericellular subcategory of Mankin scoring to determine if changes in the pericellular structure demonstrated similar trends to that of collagen VI and aggrecan neo-epitope expression levels across loading conditions. The pericellular category ranges from 0 (representing normal) to 2 (representing intensely enhanced Safranin-O/Fast Green pericellular label, indicative of PCM degradation) and contributes to the global Mankin scoring out of 10.[23,24] The two observers' subscores of the pericellular category were extracted and averaged. Pericellular Mankin scores were compared between the 2N and 3.5N loading cases at Day 15 (n = 4 rats/group) by one-way ANOVA and subsequent post hoc Tukey tests ($\alpha = 0.05$). Pericellular Mankin scores were separately compared between Day 8 and Day 15 experimental groups of the 3.5N-loaded, persistent pain condition.

3 | RESULTS

3.1 | Mechanical reflex testing assessment for behavioral sensitivity

Head withdrawal thresholds did not differ between the resolving (2N) and persistent (3.5N) pain conditions on Days 1, 3, and 5 during the loading period, as well as after the loading period on Days 7 and 9 ($p > 0.05$) (Figure 2). However, on Days 11, 13, and 14 after loading, withdrawal thresholds were higher for the 2N condition, indicating lower TMJ pain sensitivity ($p < 0.0001$) (Figure 2). Further, there was no significant difference between the 3.5N-loaded animals with tissue harvested at Day 8 and Day 15 (Figure S2), indicating consistency across groups exposed to 3.5N TMJ overloading.

3.2 | Collagen VI expression and pericellular width measurement

The amount of collagen VI increased in 3.5N-loaded TMJs on Day 15 (13.59% ± 2.68%) compared to normal (8.31% ± 2.66%; $p = 0.042$) (Figure 3). The area percent of collagen VI also increased in 2N-loaded TMJs on Day 15 (16.46% ± 3.60%) compared to normal ($p = 0.003$) (Figure 3). No changes in collagen VI were identified between the 2N and 3.5N load at Day 15 ($p = 0.323$). PCM widths, measured with the guidance of collagen VI staining, for 3.5N-loaded TMJs (2.99 μm ± 0.18, $p = 0.002$) and 2N-loaded TMJs (3.28 μm ± 0.44, $p < 0.001$) both indicated expansion of pericellular region over normal widths (2.00 ± 0.33) (Figure 5). Separately, collagen VI expression at an earlier Day 8 timepoint within the persistent pain, the 3.5N-loaded group was not statistically different than that of unloaded controls (Figure S3).

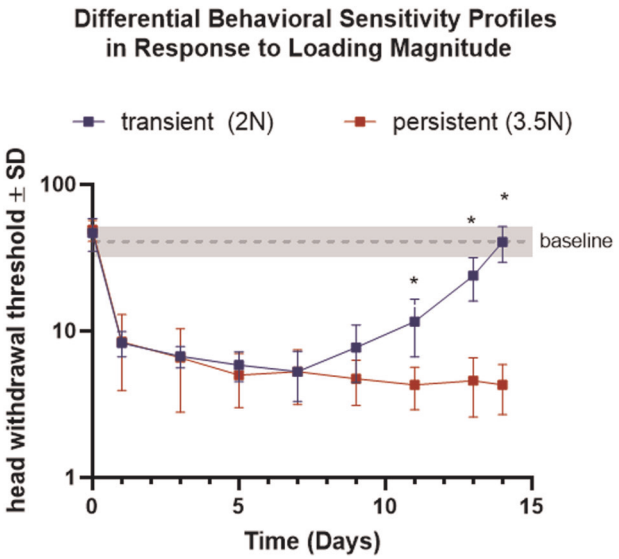

FIGURE 2 Jaw overloading magnitude corresponds to distinct behavioral sensitivity profiles. In rats used for the pericellular structural assays ($n = 7$/group), head withdrawal threshold differs between 2N- and 3.5N-loaded joints on Days 11, 13, and 14 (*). The gray line represents the baseline threshold (42.29 ± 7.96) of unloaded, matched animals [Color figure can be viewed at wileyonlinelibrary.com]

3.3 | Aggrecan neo-epitope expression

The percent positive pixels for NITEGE aggrecan neo-epitope increased in both 2N (13.52% ± 6.74%) and 3.5N (24.29% ± 5.65%) loaded TMJs at Day 15 over normal baseline (4.86% ± 1.99%, $p = 0.048$ and $p < 0.001$, respectively) (Figure 4). Additionally, in contrast to collagen VI expression, there was a significant increase in expression from the 2N-loaded group to the 3.5N-loaded paradigm ($p = 0.041$).

3.4 | Pericellular Mankin scoring

There were no significant differences in the average pericellular Mankin score (out of a possible maximum of 2) identified in Day 15 3.5N-loaded (0.84 ± 0.71, $p = 0.239$) or Day 15 2N-loaded TMJs (0.25 ± 0.09, $p = 0.999$) compared to normal control TMJs (0.25 ± 0.40) (Figure 6). Additionally, no significant differences in the average score were found when comparing Day 15 resolving, 2N-loaded versus persistent, 3.5N-loaded pain models ($p = 0.24$) (Figure 6). This corresponds with previously reported average global Mankin scorings (out of a possible maximum of 10) of 4.10 ± 0.37 in Day 15, 3.5N-loaded samples, which was greater than that of normal control (1.71 ± 0.64) as well as of Day 15, 2N-loaded TMJ sample group (2.1 ± 0.92).[34] Within the persistent pain condition, there was no significant difference of pericellular Mankin scores between Day 8, 3.5N-loaded TMJ samples compared to normal or Day 15 TMJ samples (Figure S4).

4 | DISCUSSION

This study identified increased collagen VI (Figure 3) and aggrecan neo-epitope expression by Day 15 (Figure 4) in both resolving (2N-loaded) and persistent (3.5N-loaded) pain behavior conditions of a tunable TMJ overloading model (Figure 2). Collagen VI expression increased in both 2N- and 3.5N-loaded TMJs by Day 15 (Figure 3), and aggrecan neo-epitope expression was increased more extensively within 3.5N-loaded samples compared to that of 2N-loaded TMJs (Figure 4). Our results show the degree of aggrecan fragmentation may be dependent on overloading magnitude that induce differential pain responses (Figure 4); whereas the increase in collagen VI above normal levels is similar in both loading conditions (Figure 4). This suggests aggrecan fragmentation could be used to differentiate pain responses and severity of biochemical changes characteristic of early TMJ-OA. These findings also suggest that different structural components of the PCM have variable responses

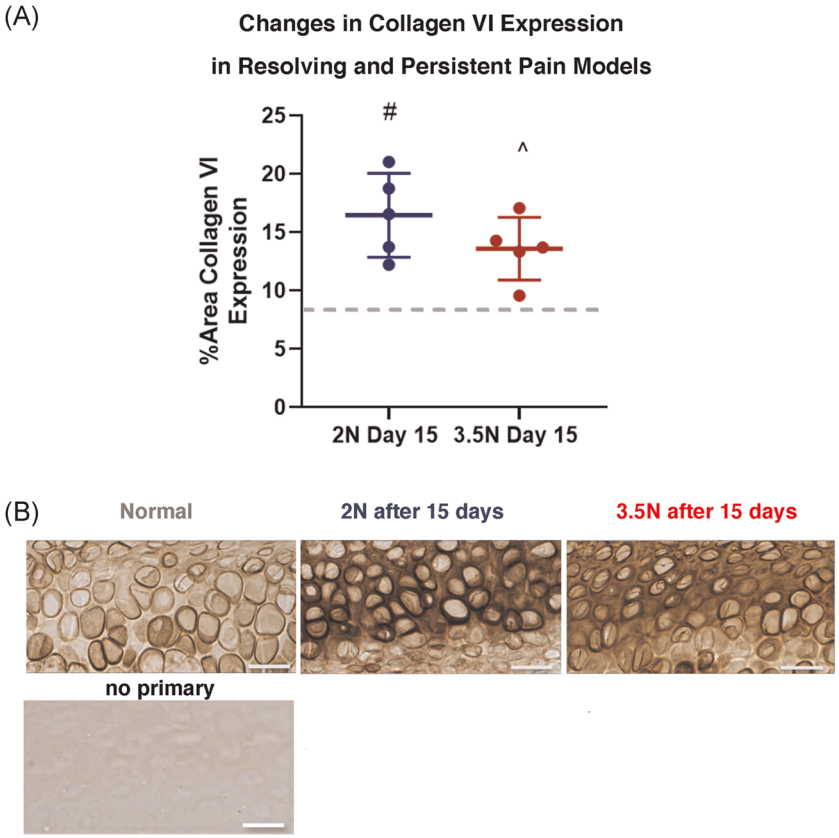

FIGURE 3 Collagen VI increases similarly in both resolving and persistent models by Day 15. (A) Collagen VI levels increased in both 2N-loaded (#) and 3.5N-loaded samples (^) by Day 15 timepoint compared to normal levels (gray dashed line). There was no significant difference between the two Day 15 experimental groups, regardless of load magnitude. (B) Corresponding DAB-IHC collagen VI labeling of hypertrophic chondrocytes acquired from normal versus resolving and persistent TMJ pain models. Compared to normal controls, both Day 15 groups have dark collagen VI pericellular labeling and diffuse expression into the interterritorial region of the tissue matrix. Scale bar = 25 μm. DAB, 3,3′-Diaminobenzidine; IHC, immunohistochemistry; TMJ, temporomandibular joint [Color figure can be viewed at wileyonlinelibrary.com]

to mechanical loading of the TMJ fibrocartilage and some aspects of those microstructural changes are observed even for cases when orofacial pain resolves.

Increases in collagen VI are observed regardless of loading magnitude (Figure 3A). Under normal, non-loaded conditions, collagen VI localizes as thin pericellular rings. In both loading conditions at Day 15, the marker appears more densely concentrated within a pericellular region compared to controls as well as more dispersed throughout the peripheral regions of the tissue matrix (Figure 3B). An increase in collagen VI is thought to be an early defensive mechanism against chondrocyte apoptosis, propagation of the inflammatory response, and catabolic degradation.[28,29] Further, early hypoxia induces upregulation of endoplasmic reticulum (ER) stress markers, causing increased secretion of ER-produced proteins[44] including collagens. Similarly, collagen VI may increase in this model even with early, mild inflammatory and catabolic changes (i.e., within the 2N, resolving pain condition) as a compensatory or preventative mechanism to protect against further degradative responses,[26] chondrocyte apoptosis,[26–28] or from an alternative pathomechanism.[44] Nugent et al.[44] describe cellular stress and compensatory changes leading to a challenging balance of cellular synthesis, secretion, and localization of pericellular collagen VI with increased dispersion of the protein across the tissue matrix. The finding that there is a similar expression of collagen VI in both the 2N and 3.5N loading paradigms at Day 15 is particularly interesting since previous work indicated greater expression of MMP-13 at Day 7, hypoxia inducible factor 1α (HIF-1α)/HIF2-α catabolic factors by Day 8 and tumor necrosis factor α (TNF-α) at Day 7 only for the greater magnitude (3.5N) loading condition.[2,34,35,45] Aligned with recent literature, the increase in collagen VI at Day 15 in both 2N and 3.5N loading models could be explained by compensatory phenomena under mild indicators of metabolic stress as well as by biomechanically sensitive chondrocytes attempting to maintain normal tethering to the cartilage extracellular matrix (ECM) via additional secretions when exposed to overloading conditions.[14,32,44]

Throughout the onset and progression of OA, aggrecan depletion occurs through upregulation of matrix metalloproteinases (MMPs) or aggrecanase (i.e., a disintegrin and metalloproteinase with thrombospondin motifs, ADAMTS family) proteolytic cleavage between the three globular domains of an aggrecan structure.[30,31,46–48] Before full degradation, aggrecan molecules become increasingly fragmented, with the newly cleaved pieces known as neo-epitopes.[46,49,50] The aggrecan NITEGE neo-epitope was selected for assessment since it is the most abundantly accumulated before subsequent total aggrecan loss.[46,47] Moreover, this production of this aggrecan fragment precedes the upregulation of other neo-epitopes such as VDIPEN[47,51] and is directly cleaved by aggrecanases as opposed to MMPs, making it a useful primary marker for early OA. Its accumulation also reveals the presence of ADAMTS-family catabolic factors, which have not been previously characterized in this model.[2]

Aggrecan NITEGE neo-epitope levels increased over normal levels by Day 15 in both the resolving and persistent pain cases (Figure 4) suggesting that ADAMTS-family aggrecanases activate

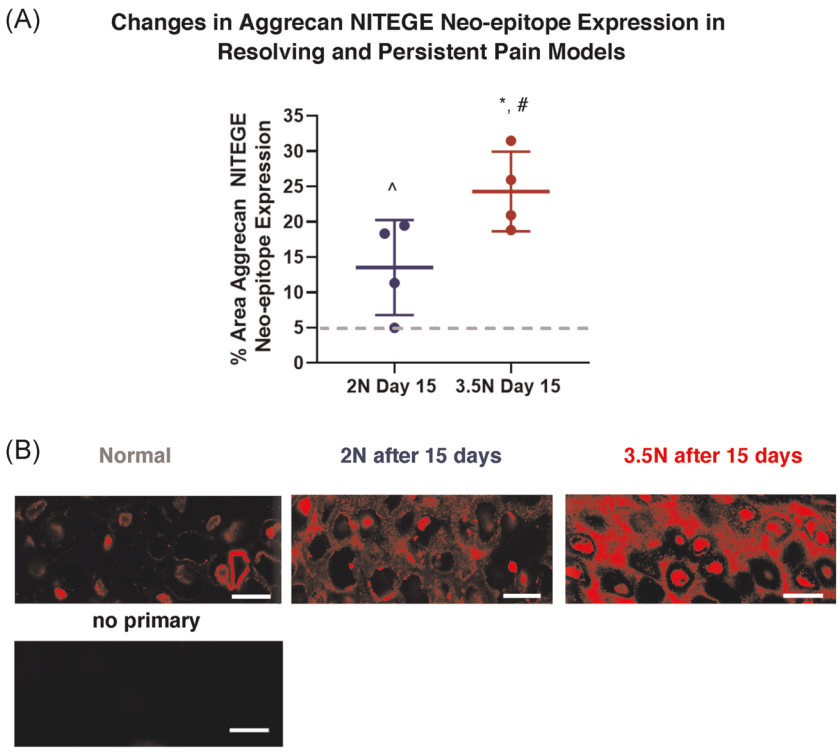

FIGURE 4 Aggrecan NITEGE neo-epitope expression gradually and directly increases dependent on load magnitude. (A) Aggrecan neo-epitope increased in both 2N-loaded (^) and 3.5N-loaded (*) TMJs on Day 15 over normal (represented by gray dashed line). Additionally, cleaved aggrecan expression was greater in 3.5N over 2N-loaded TMJs at Day 15 timepoint (#). (B) Corresponding IF images of aggrecan NITEGE neo-epitope labeled hypertrophic chondrocytes. Compared to normal, unloaded samples, where NITEGE is lightly labeled in the pericellular region and confined locally to the cell, Day 15 loaded samples had increased darkness of label in the pericellular and interterritorial regions of the tissue matrix. Day 15, 3.5N-loaded samples of the persistent paradigm appear darker with more concentrated NITEGE label in comparison to Day 15, 2N-loaded samples of the resolving model. Scale bar = 15 μm. TMJ, temporomandibular joint [Color figure can be viewed at wileyonlinelibrary.com]

and affect the structural architecture of the TMJ in pain. However, in contrast to the collagen VI expression results (Figure 3), the neo-epitope levels are greater in the persistently painful 3.5N-loaded group than in the resolving pain 2N-loaded samples (Figure 4A). The progressive increase in expression with increasing loading magnitude is similar to trends observed for MMP-13 and HIF1α/HIF2α catabolic factors at earlier timepoints.[2,35] This similarity of expression related to load magnitude may be evidence of these catabolic factors' influences on aggrecan NITEGE fragmentation in this model. Since these catabolic factors have been shown to regulate the activity of MMP/ADAMTS and subsequent proteoglycan cleavage,[2,30,31,46–53] these findings suggest that the previously studied catabolic factors may more directly impact the proteolytic cleavage pathway represented in aggrecan neo-epitope expression in comparison to collagen VI upregulation. Yet, the specific mechanistic pathways that direct the contrasting expression patterns between collagen VI and aggrecan neo-epitope in this model are still unknown.

Aggrecan neo-epitope not only increased with TMJ loading, but also underwent a shift of localization of NITEGE in mechanically loaded TMJ tissue distinct from normal TMJs. In control hypertrophic chondrocytes, the NITEGE neo-epitope was present as pericellular rings as well as intracellular fragments (Figure 4B). In tissue exposed to 2N and 3.5N loading protocols NITEGE is progressively more present and distributed in the pericellular to extracellular matrices (Figure 4B). Other models investigating chondrocyte contents have identified that aggrecan G1 domains are indeed present intracellularly and contribute to intracellular trafficking before secretion.[54,55] The difference in localization and distribution between controls and loaded samples could be attributed to stress-induced cellular disruption and dysregulated aggrecan catabolism.[54] The upregulation of catabolic activity (evident with MMP-13 and HIFs) and proteolytic cleavage (via ADAMTS) of aggrecan in the loaded models may prevent normal intracellular NITEGE epitope expression and activity. Further, in this increasingly hostile, catabolic microenvironment of the presented models, the chondrocyte and surrounding tissue complex may lose stability and endocytosis capabilities.[54] In turn, the aggrecan neo-epitope fragments become congregated within the pericellular and extracellular matrices.[54] Alternatively, it is possible that intracellular aggrecan neo-epitope labeling results from nonspecific sticking of antibody to existing intracellular nucleic acids; however, this rationale needs to be explored further by testing different immunohistochemical labeling techniques.

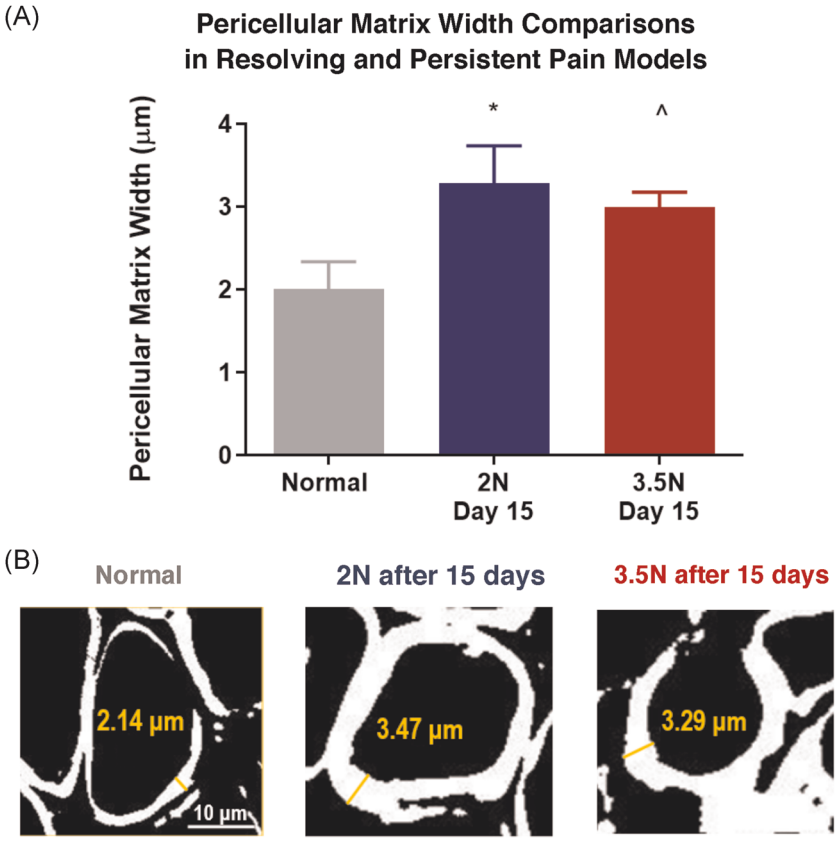

FIGURE 5 Pericellular width of TMJ chondrocytes expands following 2N or 3.5N loading at Day 15. (A) PCM width for 3.5N-loaded TMJs and 2N-loaded TMJs both indicated expansion of pericellular region over normal ($^p = 0.002$ and $^*p < 0.001$, respectively) by Day 15 timepoint. Both experimental groups averaged approximately 3 μm versus normal baseline of 2 μm. (B) Representative bi-filtered images used for pericellular width measurements with thickening of collagen VI guidance marker in both loading paradigms at Day 15 compared to normal controls. Scale bar = 10 μm. PCM, pericellular matrix; TMJ, temporomandibular joint [Color figure can be viewed at wileyonlinelibrary.com]

Aggrecan neo-epitope presence in both intracellular and pericellular regions in normal chondrocytes (Figure 4) contrasts with collagen VI localization, which solely appears as pericellular rings (Figure 3). This difference furthers the concept that these two molecular components, although both pivotal to PCM structural integrity, vary in localization, have separate roles throughout the chondron unit and ECM, and may be potentially influenced by differing catabolic pathways. This is not surprising as the two biomarkers are intrinsically different: collagen VI primarily serves as a structural network protein,[14,15,32] whereas aggrecan neo-epitope is a degradation product of a proteoglycan protein functioning to retain hydration.[16–19] By establishing unique patterns of pericellular collagens and proteoglycans, we can begin to understand each structure's properties, potentially informative to each biomolecules' functions within the PCM. Furthermore, with identifying variable expression trends of these pericellular structures, there is clear evidence of a dynamic and sensitive PCM environment within these painful overloading conditions. These are critical findings because they establish detailed microstructural alterations indicative of early osteoarthritic degeneration and align with human data on pericellular reorganization,[56] which highlights the clinical relevance of our model.

This investigation utilized collagen VI to quantify pericellular width expansion, a technique previously cited to determine PCM edges and indicative of the regional structural integrity.[32] The PCM width results within this overloading model align with collagen VI expression levels within resolving (2N) and persistent (3.5N) conditions by Day 15 in that both loaded groups experienced a similar degree of PCM expansion compared to non-loaded controls (Figure 5). Even with evidence of early inflammatory and catabolic upregulation (Day 7/Day 8) and subsequent structural reorganization (Day 15), our investigation reveals the pericellular expansion is subtle at an average of 3 μm for both conditions compared to a normal chondrocyte PCM width average of 2 μm and does not exceed 4 μm characteristic of advanced, degenerative OA.[21] PCM thickness of <4 μm suggests that loading induces an early-to-moderate OA pathology by Day 15, which generally agrees with previous global Mankin scores of approximately 4 on a 10-point grading scale for this model.[34] Accordingly, the pericellular width analysis generally corroborates our previous categorization of the tunable overloading model producing *early* indications of progressive structural degradation.

Previous studies using global Mankin scoring of the TMJ cartilage structure found that overall changes (measured via overall glycosaminoglycan, proteoglycan, and collagen content) were evident at Day 15 only in TMJs exposed to 3.5N loading.[34] However, the presented pericellular Mankin sub-scoring suggests there were no evident changes in the pericellular region between loading groups (Figure 6). Investigation of PCM-specific markers reveals pericellular microstructural changes and pericellular reorganization for both loading magnitudes, which were undetected by pericellular Mankin sub-scoring. The collagen VI and aggrecan neo-epitope assays also show changes associated with 2N-loading that were not observed by the global Mankin system (Figures 3 and 4). These differences

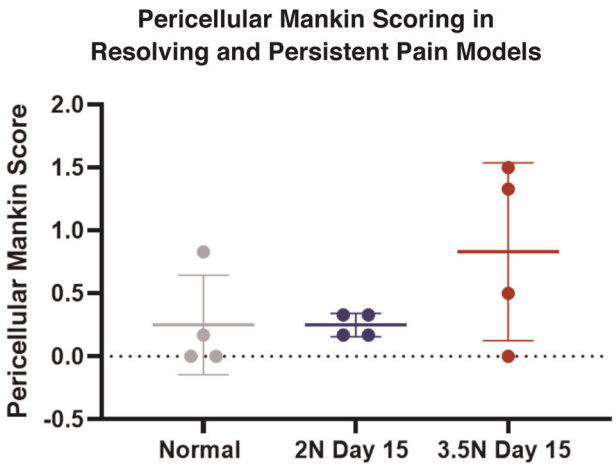

FIGURE 6 Pericellular Mankin sub-scoring does not detect changes either resolving or persistent pain models at Day 15. Unlike the previously reported global Mankin score findings, which detected macrostructural change within 3.5N-loaded TMJs at Day 15,[34] the pericellular Mankin sub-scoring did not detect any significant changes among experimental groups and compared to unloaded controls. TMJ, temporomandibular joint [Color figure can be viewed at wileyonlinelibrary.com]

suggest that individual PCM markers may provide more details in the structural degradation associated with *early* TMJ-OA and may be a more sensitive detection tool over Mankin scoring to distinguish structural remodeling of TMJs present in both persistent and resolving symptomatic pain.

This study's use of immunohistochemical evaluation to determine pericellular structural changes in the TMJ is limited in several ways. With this approach, it is challenging to accurately assess pericellular remodeling across different depths of heterogeneous tissue due to the compacted, fibrous morphology of the TMJ's superficial layers. IHC assays are also limited in demonstrating functional changes in tissue mechanical properties. Since understanding the heterogeneous architecture of the TMJ and measuring functional outcomes from tissue overloading are areas of interest, performing Atomic Force Microscopy (AFM) on TMJ fibrocartilage from our model could be a useful future approach to determine mechanical outcomes relative to tissue depth or magnitude of overloading.[57–59] Furthermore, although pain, inflammation, and catabolic factors are upregulated in the 3.5N TMJ loading case on, or before, Day 8,[2,34,35,45] the findings of this study reveal detailed pericellular microstructural changes within *both* loading conditions at Day 15 after the loading period that were previously undetected. Our preliminary assessment indicated no increases in collagen VI expression nor significant changes in pericellular Mankin scoring at Day 8 for the more aggressive, 3.5N-loaded condition, which provided rationale to focus on Day 15 outcomes (Figures 3 and 4). However, additional time course studies for both PCM markers within each pain condition are needed to define the temporal relationships between the onset of pain, inflammation, and catabolic cascades and pericellular structural outcomes. Additional limitations of this study include the differences of immunohistochemical techniques applied on collagen VI versus aggrecan NITEGE quantification (Figure S1) and the inherent subjectivity of manual analysis for both pericellular Mankin scoring and pericellular width analysis. Improvements to mitigate these limitations include standardizing IHC protocols for both pericellular markers and automating pericellular width tabulations to minimize any subjectivity.

In summary, this study bridges previously determined inflammatory and behavioral outcomes of a TMJ overloading model with tunable pain conditions to detailed pericellular structural modulations within TMJ cartilage tissue. Our hypothesis of increased pericellular structural remodeling in painful, overloaded TMJs is accepted since there are increased levels of collagen VI under both loading paradigms and progressively increased aggrecan neo-epitope in the persistent pain condition. Collagen VI and aggrecan NITEGE neo-epitope respond to overloading associated with both resolving or persistent pain expression, but with differing patterns, underscoring the complexities of pericellular structural molecules and the dynamic nature of the PCM region. The increase in collagen VI and aggrecan neo-epitope as well as pericellular width expansion is characteristic of early-to-moderate osteoarthritic development. Unlike studying the tissue matrix surrounding chondrocytes using global stains and pericellular sub-scorings, our investigation highlights the potential importance of assessing the PCM remodeling with specific markers as it provides more detailed information about tissue outcomes that could be beneficial to the characterization and diagnosis of TMJ-OA.

ACKNOWLEDGMENTS

This project was funded by the Catherine D. Sharpe Foundation, Oral and Maxillofacial Surgery Foundation, Oral and Maxillofacial Surgery Schoenleber Research Fund from the University of Pennsylvania School of Dental Medicine, a training grant from NIH/NIAMS (T32-AR007132), and a grant from the National Science Foundation (#1826202). The study sponsors had no role in study design, collection, analysis and interpretation of data; in the writing of the manuscript; and in the decision to submit the manuscript for publication. The authors would like to extend thanks to the University of Pennsylvania's Center for Musculoskeletal Diseases and Penn Microscopy Core for training and equipment use.

CONFLICT OF INTERESTS

Dr. Granquist is a consultant for Zimmer Biomet but has no conflict. The authors declare no potential conflicts of interest with respect to the authorship and/or publication of this article.

AUTHOR CONTRIBUTIONS

Melissa Franklin and Megan M. Sperry developed the approach and designed the experiments. Melissa Franklin implemented the experiments, performed analyses, and interpreted data with supervision from Megan M. Sperry. Evan Phillips developed protocols for data analysis and assisted with data interpretation. Eric J. Granquist

helped supervise the project, provided a clinical framework and funding support. Michele Marcolongo and Beth A. Winkelstein conceived and guided the original project ideas and provided funding support. Melissa Franklin wrote the manuscript with support and editing from Megan M. Sperry, Michele Marcolongo, and Beth A. Winkelstein. All authors discussed the results and provided critical feedback that shaped the research and the manuscript.

ORCID

Melissa Franklin https://orcid.org/0000-0001-9015-7324
Megan M. Sperry http://orcid.org/0000-0001-8310-5358
Beth A. Winkelstein http://orcid.org/0000-0003-0414-0484

REFERENCES

1. Praveena K, Rathika R, Easwaran M, Easwaran B. Temperomandibular disorders Clinical and Modern Method In Differential Diagnosis. *IOSR-JDMS*. 2014;13(9):1-7.
2. Kartha S, Zhou T, Granquist EJ, Winkelstein BA. A rat model of tunable TMJ pain, inflammation & condylar degeneration. *J Oral Maxillofac Surg*. 2016;74(1):54.
3. Wadhwa S, Kapila S. TMJ disorders: future innovations in diagnostics and therapeutics. *AADS Proc*. 2008;72(8):930-947.
4. Das SK. TMJ osteoarthritis and early diagnosis. *J Oral Biol Craniofac Res*. 2013;3(3):109-110.
5. Wang XD, Zhang JN, Gan YH, Zhou YH. Current understanding of pathogenesis and treatment of TMJ osteoarthritis. *J Dent Res*. 2015;94(5):666-673.
6. Yount K. Osteoarthritis of the temporomandibular joint. *Pract Pain Manag*. 2011;3(4).
7. Chantaracherd P, John MT, Hodges JS, Schiffman EL. Temporomandibular joint disorders' impact on pain, function, and disability. *J Dent Res*. 2015;94(3):79-86.
8. Stegenga B, de Bont LG, Boering G. Osteoarthrosis as the cause of craniomandibular pain and dysfunction: a unifying concept. *J Oral Maxillofac Surg*. 1989;47(3):249-256.
9. Tanaka E, Detamore MS, Mercuri LG. Degenerative disorders of the temporomandibular joint: etiology, diagnosis, and treatment. *J Dent Res*. 2008;87(4):296-307.
10. Madden R, Han SK, Herzog W. Chondrocyte deformation under extreme tissue strain in two regions of the rabbit knee joint. *J Biomech*. 2013;46(3):554-560.
11. Nguyen BV, Wang Q, Kuiper NJ, El Haj AJ, Thomas CR, Zhang Z. Strain-dependent viscoelastic behaviour and rupture force of single chondrocytes and chondrons under compression. *Biotechnol Lett*. 2009;31(6):803-809.
12. Guilak F, Ratcliffe A, Mow AC. Chondrocyte deformation and local tissue strain in articular cartilage: a confocal microscopy study. *J Orthop Res*. 1995;13(3):410-421.
13. Choi JB, Youn I, Cao L, et al. Zonal changes in the three-dimensional morphology of the chondron under compression: the relationship among cellular, pericellular, and extracellular deformation in articular cartilage. *J Biomech*. 2007;40(12):2596-2603.
14. Cescon M, Gattazzo F, Chen P, Bonaldo P. Collagen VI at a glance. *J Cell Sci*. 2015;128:3525-3531.
15. Guilak F, Alexopoulos LG, Uptom ML, et al. The pericellular matrix as a transducer of biomechanical and biochemical signals in articular cartilage. *Ann N Y Acad Sci*. 2006;1068:498-512.
16. Iozzo RV, Schaefer L. Proteoglycan form and function: a comprehensive nomenclature of proteoglycans. *Matrix Biol*. 2015;42:11-55.
17. Dean D, Han L, Grodzinsky AJ, Ortiz C. Compressive nanomechanics of opposing aggrecan macromolecules. *J Biomech*. 2006;39(14):2555-2565.
18. Seog J, Dean D, Plaas AHK, Wong-Palms S, Grodzinsky AJ, Ortiz C. Direct measurement of glycosaminoglycan intermolecular interactions via high-resolution force spectroscopy. *Macromolecules*. 2002;35(14):5601-5615.
19. Buschmann MD, Grodzinsky AJ. A molecular model of proteoglycan associated electrostatic forces in cartilage mechanics. *J Biomech Eng*. 1995;117(2):179-192.
20. Khoshgoftar M, Torzilli P, Maher S. Influence of the pericellular and extracellular matrix structural properties on chondrocyte mechanics. *J Orthop Res*. 2017;36(2):721-729.
21. Guilak F, Nims RJ, Dicks A, Wu CL, Meulenbelt I. Osteoarthritis as a disease of the cartilage pericellular matrix. *Matrix Biol*. 2018;71-72:40-50.
22. Pauli C, Whiteside R, Heras FL, et al. Comparison of cartilage histopathology assessment systems on knee joints at all stages of osteoarthritis development. *Osteoarthr Cartil*. 2012;20(6):476-485.
23. Xu L, Polur I, Lim C, et al. Early-onset osteoarthritis of mouse temporomandibular joint induced by partial discectomy. *Osteoarthr Cartil*. 2009;17(7):917-922.
24. Shen P, Jiao Z, Zheng JS, et al. Injecting vascular endothelial growth factor into the temporomandibular joint induces osteoarthritis in mice. *Sci Rep*. 2015;5:16244.
25. Van der Slujis JA, Geesink RJ, van der Linden AJ. The reliability of the Mankin score for osteoarthritis. *J Orthop Res*. 1992;10(1):58-61.
26. Hambach L, Neureiter D, Zeiler G. Severe disturbance of the distribution and expression of type VI collagen chains in osteoarthritic articular cartilage. *Arthritis Rheum*. 1998;41(6):986-996.
27. Pullig O, Weseloh G, Swoboda B. Expression of type VI collagen in normal and osteoarthritic human cartilage. *Osteoarthr Cartil*. 1999;7(2):191-202.
28. Chu WC, Zhang S, Sng TJ, et al. Distribution of pericellular matrix molecules in the temporomandibular joint and their chondroprotective effects against inflammation. *Int J Oral Sci*. 2017;9(1):43-52.
29. Peters HC, Otto TJ, Enders JT, Jin W, Moed BR, Zhang Z. The protective role of the pericellular matrix in chondrocyte apoptosis. *Tissue Eng Part A*. 2011;17(15–16):2017-2024.
30. Hardingham T, Fosang A. Proteoglycans: many forms and many functions. *FASEB J*. 1992;6(3):861-870.
31. Roughley PJ, Mort JS. The role of aggrecan in normal and osteoarthritic cartilage. *J Exp Orthop*. 2014;1(1):8.
32. Zelenski NA, Leddy HA, Sanchez-Adams J, et al. Type VI collagen regulates pericellular matrix properties, chondrocyte swelling, and mechanotransduction in mouse articular cartilage. *Arthritis Rheumatol*. 2015;67(5):1286-1294.
33. Alexopoulos LG, Youn I, Bonaldo P, Guilak F. Developmental and osteoarthritic changes in Col6a1-knockout mice: biomechanics of type VI collagen in the cartilage pericellular matrix. *Arthritis Rheumatol*. 2009;60(3):771-779.
34. Sperry MM, Yu Y, Welch R. Grading facial expression is a sensitive means to detect grimace differences in orofacial pain in a rat model. *Sci Rep*. 2018;8:13894.
35. Sperry MM, Yu YH, Kartha S, et al. Intra-articular etanercept attenuates pain and hypoxia from TMJ loading in the rat. *J Orthop Res*. 2020;38:1316-1326. https://doi.org/10.1002/jor.24581
36. Institute for Laboratory Animal Research. *Guide for the Care and Use of Laboratory Animals*, 8th ed.; 2011. https://doi.org/10.2307/1525495. https://grants.nih.gov/grants/olaw/guide-for-the-care-and-use-of-laboratory-animals.pdf
37. Zimmermann M. Ethical guidelines for investigations of experimental pain in conscious animals. *Pain*. 1983;16(2):109-110.
38. Nicoll SB, Hee CK, Davis MB, et al. A rat model of temporomandibular joint pain with histopathologic modifications. *J Orofac Pain*. 2010;24:298.

39. Zhang L, Hu J, Athanasiou KA. The role of tissue engineering in articular cartilage repair and regeneration. *Crit Rev Biomed Eng*. 2009;37(1–2):1-57.
40. Dreier R. Hypertrophic differentiation of chondrocytes in osteoarthritis: the developmental aspect of degenerative joint disorders. *Arthritis Res Ther*. 2010;12(5):216.
41. Embree M, Ono M, Kilts T, et al. Role of subchondral bone during early-stage experimental TMJ osteoarthritis. *J Dent Res*. 2011; 90(11):1331-1338.
42. Kuroda S, Tanimoto K, Izawa T, Fujihara S, Koolstra JH, Tanaka E. Biomechanical and biochemical characteristics of the mandibular condylar cartilage. *Osteoarthr Cartil*. 2009;17(11):1408-1415. https://doi.org/10.1016/j.joca.2009.04.025
43. Phillips ER, Haislup BD, Bertha N, et al. Biomimetic proteoglycans diffuse throughout articular cartilage and localize within the pericellular matrix. *J Biomed Mater Res*. 2019;107(9):1977-1987.
44. Nugent AE, Speicher DM, Gradisar I, et al. Advanced osteoarthritis in humans is associated with altered collagen VI expression and upregulation of ER-stress markers Grp78 and Bag-1. *J Histochem Cytochem*. 2009;57(10):923-931.
45. Sperry MM, Stiansen N, Ghimire P, et al. Repeated, painful jaw overloading activates osteoclasts & remodels the trabecular architecture of the TMJ condyle. *8th World Congress of Biomechanics Conference Proceeding*; 2018.
46. Janusz MJ, Little CB, King LE, et al. Detection of aggrecanase- and MMP-generated catabolic neoepitopes in the rat iodoacetate model of cartilage degeneration. *Osteoarthr Cartil*. 2004;12(9):720-728.
47. Nagase H, Kashiwagi M. Aggrecanases and cartilage matrix degradation. *Arthritis Res Ther*. 2003;5(2):94-103.
48. Ghassemi-Nejad S, Kobezda T, Rauch TA, Matesz C, Glant TT, Mikecz K. Osteoarthritis-like damage of cartilage in the temporomandibular joints in mice with autoimmune inflammatory arthritis. *Osteoarthr Cartil*. 2011;19(4):458-465.
49. van Meurs JBJ, van Lent PLEM, Holthuysen AEM, Singer II, Bayne EK, Van Den Berg WB. Kinetics of aggrecanase- and metalloproteinase-induced neoepitopes in various stages of cartilage destruction in murine arthritis. *Arthritis Rhumatol*. 2001;42(6): 1128-1139.
50. Tortorella M, Pratta M, Fox J, Arner E. The interglobular domain of cartilage aggrecan is cleaved by hemorrhagic metalloproteinase HT-d (Atrolysin C) at the matrix metalloproteinase and aggrecanase sites. *J Biol Chem*. 1998;273:5846-5850.
51. Leonardi R, Crimi S, Almeida LE, et al. ADAMTS-4 and ADAMTS-5 expression in human temporomandibular joint discs with internal derangement, correlates with degeneration. *J Oral Pathol Med*. 2015; 44(10):870-875.
52. Fujita H, Morisugi T, Tanaka Y, Kawakami T, Kirita T, Yoshimura Y. MMP-3 activation is a hallmark indicating an early change in TMJ disorders, and is related to nitration. *Int J Oral Maxillofac Surg*. 2009; 38(1):70-78.
53. Poole CA. Articular cartilage chondrons: form, function, and failure. *J Anat*. 1997;191(1):1-13.
54. Embry Flory JJ, Fosang AJ, Knudson W. The accumulation of intracellular ITEGE and DIPEN neoepitopes in bovine articular chondrocytes is mediated by CD44 internalization of hyaluronan. *Arthritis Rheumatol*. 2006;54(2):443-454.
55. Yasumoto T. The G1 domain of aggrecan released from porcine articular cartilage forms stable complexes with hyaluronan/link protein. *Rheumatology*. 2003;42(2):336-342.
56. Lotz MK, Otsuki S, Grogan SP, Sah R, Terkeltaub R, D'Lima D. Cartilage cell clusters. *Arthritis Rheum*. 2010;62(8):2206-2218. https://doi.org/10.1002/art.27528
57. Chery DR, Han B, Li Q, et al. Early changes in cartilage pericellular matrix micromechanobiology portend the onset of post-traumatic osteoarthritis. *Acta Biomater*. 2020;111:267-278. https://doi.org/10.1016/j.actbio.2020.05.005
58. Xu X, Li Z, Leng Y, Neu CP, Calve S. Knockdown of the pericellular matrix molecule perlecan lowers in situ cell and matrix stiffness in developing cartilage. *Dev Biol*. 2016;418(2):242-247. https://doi.org/10.1016/j.ydbio.2016.08.029
59. Chandrasekaran P, Doyran B, Li Q, et al. Biomechanical properties of murine TMJ articular disc and condyle cartilage via AFM-nanoindentation. *J Biomech*. 2017;60:134-141. https://doi.org/10.1016/j.jbiomech.2017.06.031

SUPPORTING INFORMATION

Additional Supporting Information may be found online in the supporting information tab for this article.

How to cite this article: Franklin M, Sperry MM, Phillips E, Granquist EJ, Marcolongo M, Winkelstein BA. Painful temporomandibular joint overloading induces structural remodeling in the pericellular matrix of that joint's chondrocytes. *J Orthop Res*. 2021;1-11. https://doi.org/10.1002/jor.25050